Stem Cell Reports
Resource
OPEN ACCESS

Nonadhesive Alginate Hydrogels Support Growth of Pluripotent Stem Cell-Derived Intestinal Organoids

Meghan M. Capeling,[1] Michael Czerwinski,[2] Sha Huang,[2] Yu-Hwai Tsai,[2] Angeline Wu,[2] Melinda S. Nagy,[2] Benjamin Juliar,[1] Nambirajan Sundaram,[3] Yang Song,[4] Woojin M. Han,[5,6] Shuichi Takayama,[4] Eben Alsberg,[7] Andres J. Garcia,[5,6] Michael Helmrath,[3,8] Andrew J. Putnam,[1] and Jason R. Spence[1,2,9,10,*]

[1]Department of Biomedical Engineering, University of Michigan College of Engineering, Ann Arbor, MI 48109, USA
[2]Department of Internal Medicine, Gastroenterology, University of Michigan Medical School, Ann Arbor, MI 48109, USA
[3]Division of Pediatric General and Thoracic Surgery Cincinnati Children's Hospital Research Foundation, Cincinnati, OH 45229, USA
[4]Wallace H. Coulter Department of Biomedical Engineering, Georgia Institute of Technology and Emory School of Medicine, Atlanta, GA 30332, USA
[5]Parker H. Petit Institute for Bioengineering and Biosciences, Georgia Institute of Technology, Atlanta, GA 30332, USA
[6]George W. Woodruff School of Mechanical Engineering, Georgia Institute of Technology, Atlanta, GA 30332, USA
[7]Department of Biomedical Engineering, Case Western Reserve University, Cleveland, OH 44106, USA
[8]Center for Stem Cell and Organoid Medicine (CuSTOM) Cincinnati Children's Hospital Research Foundation, Cincinnati, OH 45229, USA
[9]Department of Cell and Developmental Biology, University of Michigan Medical School, Ann Arbor, MI 48109, USA
[10]Center for Organogenesis, University of Michigan Medical School, Ann Arbor, MI 48109, USA
*Correspondence: spencejr@umich.edu
https://doi.org/10.1016/j.stemcr.2018.12.001

SUMMARY

Human intestinal organoids (HIOs) represent a powerful system to study human development and are promising candidates for clinical translation as drug-screening tools or engineered tissue. Experimental control and clinical use of HIOs is limited by growth in expensive and poorly defined tumor-cell-derived extracellular matrices, prompting investigation of synthetic ECM-mimetics for HIO culture. Since HIOs possess an inner epithelium and outer mesenchyme, we hypothesized that adhesive cues provided by the matrix may be dispensable for HIO culture. Here, we demonstrate that alginate, a minimally supportive hydrogel with no inherent cell instructive properties, supports HIO growth *in vitro* and leads to HIO epithelial differentiation that is virtually indistinguishable from Matrigel-grown HIOs. In addition, alginate-grown HIOs mature to a similar degree as Matrigel-grown HIOs when transplanted *in vivo*, both resembling human fetal intestine. This work demonstrates that purely mechanical support from a simple-to-use and inexpensive hydrogel is sufficient to promote HIO survival and development.

INTRODUCTION

A pivotal development in the fields of developmental biology and regenerative medicine was the use of human pluripotent stem cells (hPSCs) to generate human cell types, tissues, and organoid model systems *in vitro* (Huch et al., 2017; Johnston, 2015; Little, 2017). hPSC-derived organoids are 3-dimensional (3D) organ-like tissues that partially recapitulate structural and functional aspects of the organs after which they are modeled (Dye et al., 2015, 2016; Eiraku et al., 2011; Lancaster et al., 2013; Miller et al., 2018; Spence et al., 2011; Takasato et al., 2014; Takebe et al., 2013). In particular, human intestinal organoids (HIOs) are a useful tool to study intestinal development (Aurora and Spence, 2016; Dedhia et al., 2016; Finkbeiner et al., 2015a, 2015b; Munera et al., 2017; Singagoga and Wells, 2015; Tsai et al., 2016, 2017), evaluate gut-microbe interactions (Hill et al., 2017), and model chronic health conditions such as inflammatory bowel disease (Wells and Spence, 2014).

HIOs are generated from hPSCs through a stepwise differentiation process resulting in the formation of multicellular spheroids that are embedded in a 3D extracellular matrix (ECM) to support growth and development. Spheroids grow into HIOs over the course of approximately 30 days in culture (Spence et al., 2011). Currently, basement membrane-like ECM derived from mouse sarcoma cells, sold under brand names such as Matrigel or Cultrex, are standard for organoid culture as they mimic the basement membrane and help to support epithelial growth. There are many issues with these cell-derived ECMs, including batch-to-batch variability, inability to control biophysical and biochemical properties, and a potential for pathogen transfer (Czerwinski and Spence, 2017). Perhaps most importantly, cell-derived ECMs typically have an uncharacterized protein composition and introduce a largely uncontrollable biological variability into experimental design. Lastly, cell-derived ECMs have a high cost, hindering scale-up. Collectively, these factors limit biological control during experiments and hamper downstream clinical applications. These limitations have prompted investigation into fully defined synthetic matrices to support organoid culture *in vitro*. Thus far only polyethylene glycol (PEG) has been used for HIO culture, motivating research into other hydrogel systems. Recent work has shown that modified PEG hydrogels can be engineered to support HIO growth (Cruz-Acuna et al., 2017), or to support epithelium-only organoids (enteroids)

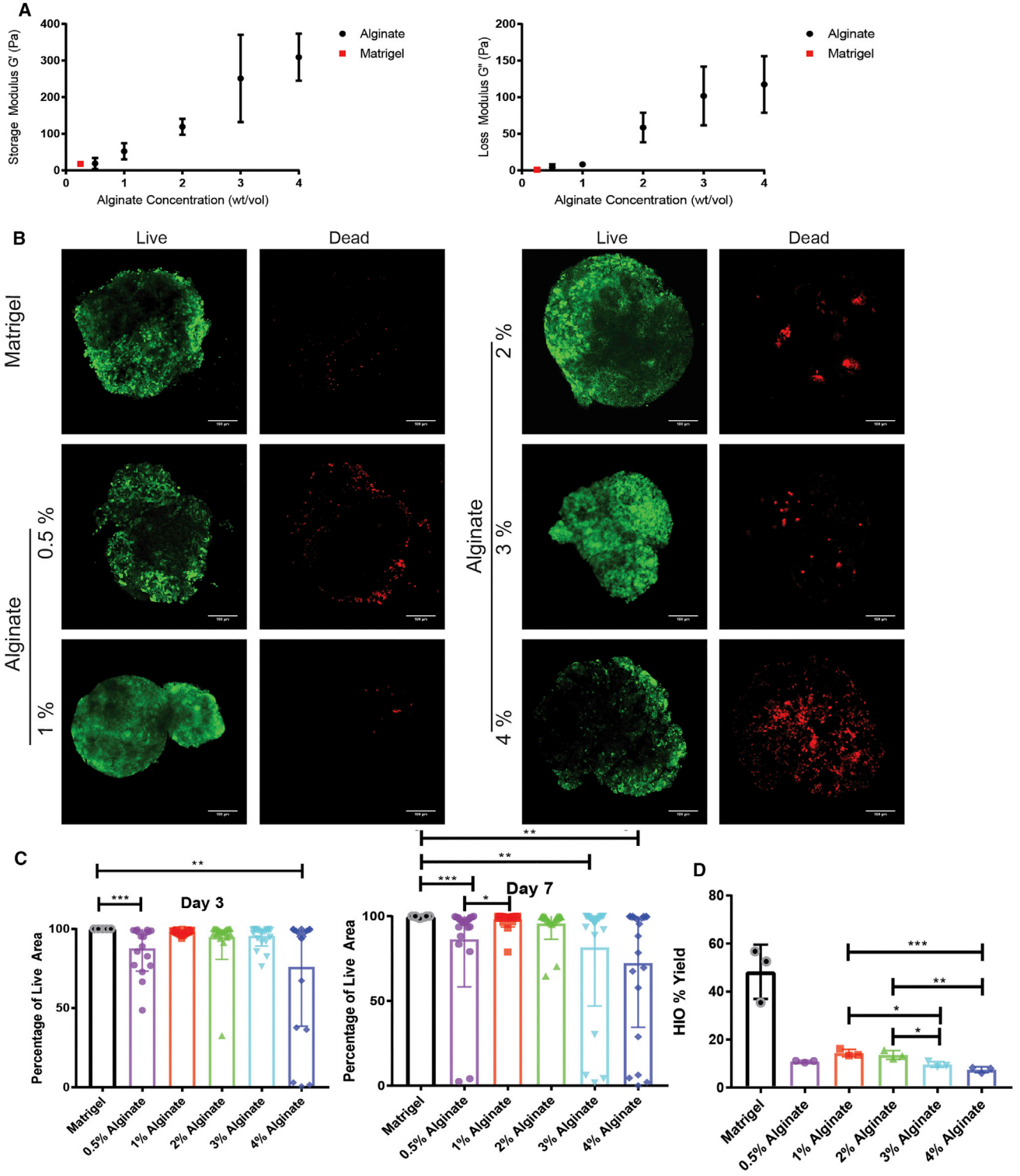

Figure 1. Alginate Supports HIO Survival *In Vitro*

(A) Rheological characterization of alginate hydrogels. Data shown are the mean ± SD from n ≥ 3 gels per condition.

(B) Representative images of live (Calcein-AM, green) and dead (Ethidium-homodimer-1, red) staining of spheroids in alginate and Matrigel after 7 days in culture. Scale bar, 100 μm.

(legend continued on next page)

generated from isolated murine or human intestinal stem cells (Gjorevski et al., 2016). These studies focused on engineering hydrogels to mimic the stiffness, adhesivity, and degradation dynamics required to support cellular viability and attachment (Cruz-Acuna et al., 2017; Gjorevski et al., 2016). However, given that hPSC-derived HIOs are composed of both epithelium and an outer mesenchyme with a supportive basement membrane, we hypothesized that HIOs may create their own niche and thus may be amenable to growth in substrates lacking inherent cell recognition.

In this work, we present evidence that native (unmodified) alginate can be used as a simple hydrogel system that supports HIO growth and development *in vitro* and transplantation *in vivo* into immunocompromised mice. Alginate is a Food and Drug Administration (FDA)–approved polysaccharide derived from algae that is favorable due to its biocompatibility and ease of manipulation. Use of alginate does not require specialized bioengineering skills, and gelation is controlled by crosslinking with calcium; thus, alginate can be implemented using commercially available reagents without a need for further modification. Since unmodified alginate does not possess cell adhesive properties and its hydrophilic nature inhibits protein adsorption, it is a minimally supportive matrix that provides mechanical support for HIOs in a 3D environment. Here, we report that alginate hydrogels supported HIO viability and development *in vitro*. HIOs cultured in alginate grew optimally at a stiffness that was comparable to previously described PEG hydrogels optimized for HIOs (Cruz-Acuna et al., 2017), and the resulting alginate-grown HIOs were highly similar to Matrigel-grown HIOs *in vitro*. Alginate and Matrigel-grown HIOs underwent similar engraftment and maturation when transplanted *in vivo*, and both closely resembled the human intestine after transplantation. Collectively, these results demonstrate the effectiveness of alginate as a support matrix for HIOs and as an alternative for cell-derived ECM. Alginate overcomes many limitations of Matrigel and is significantly more cost-effective than either Matrigel or PEG, making it a promising solution to improve experimental control and increase the clinical potential of organoids.

RESULTS

Alginate Hydrogels Support HIO Viability

We identified alginate as a potential HIO growth matrix based on its cost-effectiveness, biocompatibility, mild gelation conditions (Lee and Mooney, 2012), ability to control physical and biochemical properties (Jeon et al., 2013; Samorezov et al., 2015), and viscoelastic behavior (Webber and Shull, 2004). Many extracellular matrices and soft tissues exhibit viscoelastic behavior *in vivo* (Chaudhuri, 2017), including embryonic tissue (Forgacs et al., 1998). Previous work demonstrated that modified PEG hydrogels engineered to mimic the adhesive and biomechanical properties of Matrigel could support HIO development (Cruz-Acuna et al., 2017; Gjorevski et al., 2016); however, we hypothesized that due to the combined mesenchymal and epithelial composition of HIOs that establishes a Laminin-rich basement membrane (Arora et al., 2017; Spence et al., 2011), a simple nonadhesive hydrogel with a similar stiffness to Matrigel may also support HIO growth. Thus, we explored the potential of unmodified alginate to support HIO expansion.

After inducing hPSCs toward an intestinal lineage as previously described (Finkbeiner et al., 2015a; McCracken et al., 2011; Spence et al., 2011; Tsai et al., 2016, 2017), 3D hindgut spheroids self-assemble and detach from the 2D monolayer. These spheroids develop into HIOs over the course of approximately 30 days in 3D culture. Spheroids were collected and embedded in Matrigel or in alginate hydrogels spanning a range of polymer densities (0.5%–4% w/v). Alginate solutions containing spheroids were ionically crosslinked with a calcium chloride solution to form 3D hydrogel networks. Since matrix mechanical properties have been shown to impact HIO viability (Cruz-Acuna et al., 2017) as well as epithelial cell behavior (Enemchukwu et al., 2016), we varied the properties of alginate hydrogels by varying polymer density in order to identify an optimal matrix to support cell viability (Figure 1). Using rheometry, we measured the mechanical properties of alginate gels with an *in situ* gelation test. Rheological data confirm that both the storage and loss moduli of alginate hydrogels increase with increasing polymer density. The storage and loss moduli of 0.5% alginate were most similar

(C) Quantification of spheroid viability after 3 and 7 days encapsulated in alginate or Matrigel. Percentage of live area denotes area of spheroid expressing live marker over total spheroid area. Data are combined from three independent experiments with $n \geq 6$ spheroids per condition per experiment. Each point depicts viability of an individual spheroid, while bars depict mean and SE. Significance was calculated with a one-way ANOVA and Tukey's multiple comparisons test.

(D) Quantification of HIO yield after 28 days in culture. HIO yield was calculated as the percentage of spheroids that gave rise to HIOs. Data shown are the average yields from three independent experiments with $n > 100$ spheroids per condition. Each point depicts overall yield from one experiment, while bars depict mean and SE. Significance was calculated with a one-way ANOVA and Tukey's multiple comparisons test.

$^{*}p \leq 0.05$, $^{**}p \leq 0.01$, $^{***}p \leq 0.001$. See also Figures S1–S3.

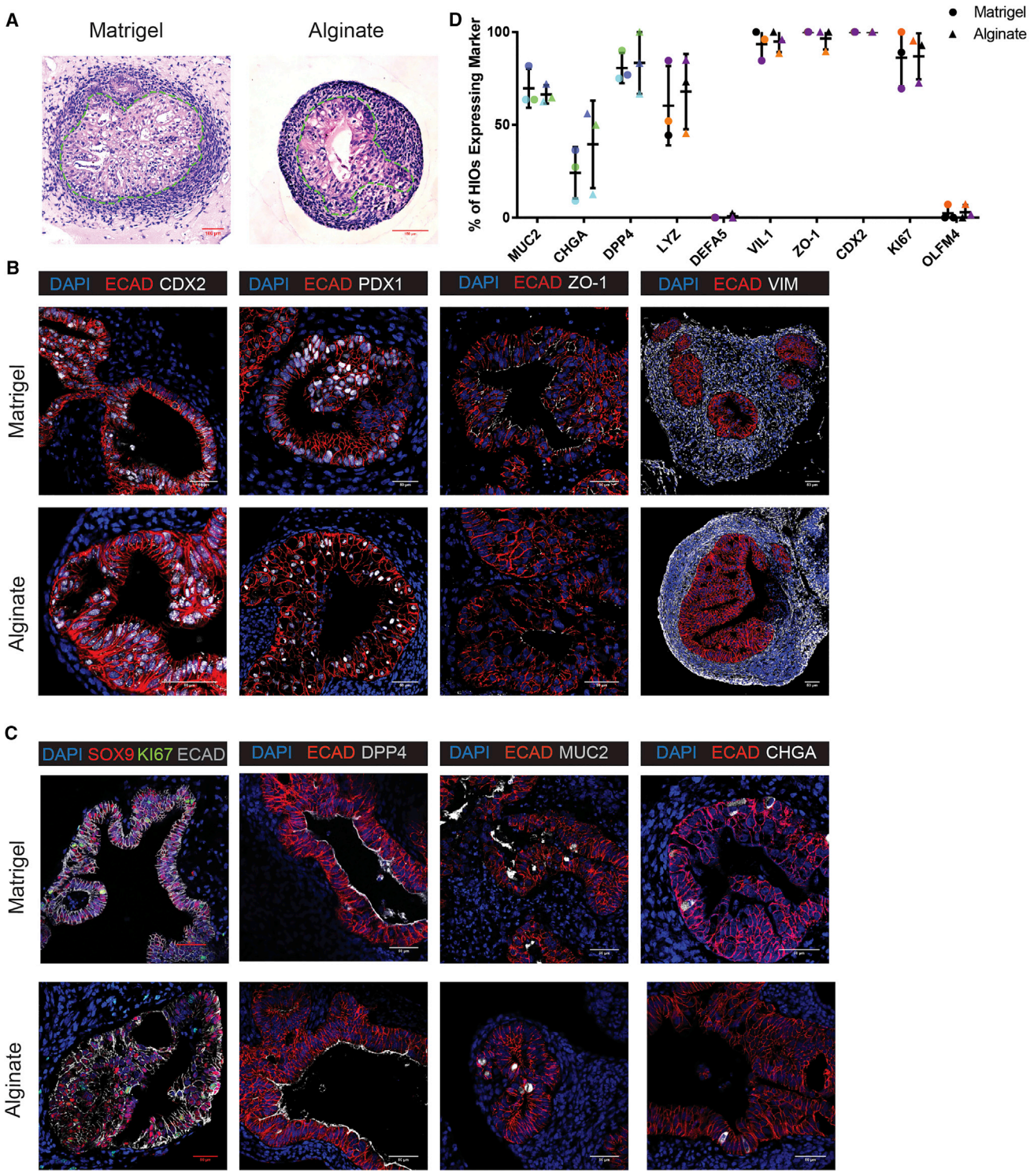

Figure 2. Epithelium of Alginate-Grown HIOs Resembles Epithelium of Matrigel-Grown HIOs *In Vitro*

(A) H&E staining of HIOs cultured in 1% alginate and Matrigel for 28 days. Dashed lines outline the epithelium.

(B) Representative images of general epithelial marker staining in HIOs cultured in 1% alginate and Matrigel for 28 days. Markers shown are ECAD (epithelial marker), CDX2 (intestinal epithelium marker), PDX1 (duodenum marker), ZO-1 (tight junction marker), and VIM (mesenchymal marker). Scale bar, 50 μm.

(legend continued on next page)

to Matrigel, while those of 1% alginate were higher than Matrigel but similar to PEG hydrogels optimized for HIO formation as reported by others (Cruz-Acuna et al., 2017) (Figure 1A).

To optimize alginate growth conditions throughout the course of HIO development, we established metrics of success at both early and late time points. We examined spheroid viability at days 3 and 7 after encapsulation to assess the initial response of spheroids to alginate (Figures 1B and 1C), as well as quantified overall HIO yield after 28 days, calculated as the percentage of embedded spheroids which matured into HIOs (Figure 1D). Using live-dead staining, HIO viability was quantified as the percentage of spheroid area live-stained at days 3 and 7 post-encapsulation. Results presented in Figure 1C represent combined data from three independent experiments where $n \geq 6$ spheroids were analyzed at each condition. At 3 days post-encapsulation, none of the Matrigel spheroids (0%) displayed signs of death, while spheroids in all concentrations of alginate displayed some cell death. After 3 days, spheroids in both 0.5% alginate and 4% alginate displayed significant decreases in viability, while spheroids in 1%, 2%, and 3% alginate displayed similar viability compared to spheroids in Matrigel (Figure 1C). We noted a highly variable degree of viability in 4% alginate with some spheroids exhibiting high viability and others exhibiting complete death. By 7 days post-encapsulation, spheroids embedded in both 1% and 2% alginate retained the highest viability and spheroids grown in 0.5%, 3%, and 4% alginate exhibited decreased average viability from day 3 to day 7 with multiple spheroids showing close to 0% viability in each of these conditions (Figure 1C). On the other hand, spheroids grown in 1% and 2% alginate remained nearly 100% viable with only a few spheroids displaying cell death. Thus, by day 7 it was apparent that spheroid survival depends on alginate density, with 1% and 2% alginate best supporting viability.

HIO yield was calculated as the percentage of spheroids at day 1 of encapsulation that gave rise to HIOs after 28 days (Figure 1D). All of the alginate concentrations tested produced significantly lower HIO yields than Matrigel, although we note that our yield in Matrigel is 3.7-fold higher than those reported by others (Arora et al., 2017). The low HIO yields at day 28 as compared with high viability in alginate at day 7 suggests that additional death may occur later in HIO development, or that certain spheroids do not expand in alginate. HIO yield was highest in 1% alginate as compared with all other alginate formulations tested, although there was no significant difference in yield between 0.5%, 1%, and 2% alginate. We selected 1% or 2% alginate as the optimal concentrations for future experiments since these concentrations resulted in the highest spheroid viability at early time points as well as highest overall HIO yield. We further encapsulated spheroids from three additional hPSC lines in Matrigel or 1% alginate and observed very similar growth between lines, resulting in HIOs with expected morphology (Figures S1A and S1B) and comparable yields between 1% alginate and Matrigel across all four lines (Figure S1C).

The Epithelium of Alginate-Grown HIOs Is Indistinguishable from Matrigel-Grown HIOs

After 28 days of culture, we used histological techniques to compare HIOs cultured in alginate and Matrigel. Histological analysis with H&E staining revealed that HIOs cultured in both alginate and Matrigel form an inner epithelium surrounded by an outer mesenchyme (Figure 2A). While the epithelium of alginate and Matrigel-grown HIOs appears quite similar histologically, the mesenchyme of Matrigel-grown HIOs invades the surrounding matrix whereas alginate-grown HIOs do not appear to invade the hydrogel.

HIOs cultured in both alginate and Matrigel were examined for the presence of markers of intestinal epithelial patterning, mesenchyme formation, and polarization (Figure 2B) as well as markers of fully differentiated intestinal cell types including enterocytes, goblet cells, and enteroendocrine cells (Figure 2C). The epithelium of both alginate and Matrigel-grown HIOs expressed the intestinal epithelial marker CDX2, confirming that alginate-grown HIOs differentiate along an intestinal lineage as observed in Matrigel-grown HIOs. In addition, both alginate and Matrigel-grown HIOs expressed the duodenum marker PDX1 throughout the epithelium, indicating that HIOs cultured in both matrices became patterned into proximal small intestine (Tsai et al., 2017). Alginate and Matrigel-grown HIOs expressed the tight junction marker ZO-1 at apical surfaces suggesting proper epithelial polarization. In addition, both alginate and Matrigel-grown HIOs

(C) Representative images of specific epithelial cell marker staining in HIOs cultured in 1% alginate and Matrigel for 28 days. Markers shown are SOX9 (progenitor cell marker), KI67 (proliferative cell marker), DPP4 (small intestinal brush border enzyme marker), MUC2 (goblet cell marker), and CHGA (enteroendocrine marker). Scale bar, 50 μm.

(D) Frequency of mature cell type differentiation in 1% alginate and Matrigel. Points depict the percentage of HIOs expressing each marker as assessed by protein staining for three independent experiments with $n \geq 6$ HIOs per experiment. Each color represents one matched experiment. Significance was calculated with a one-way ANOVA and Tukey's multiple comparisons test. Bars depict mean and SE.

See also Figures S1 and S2.

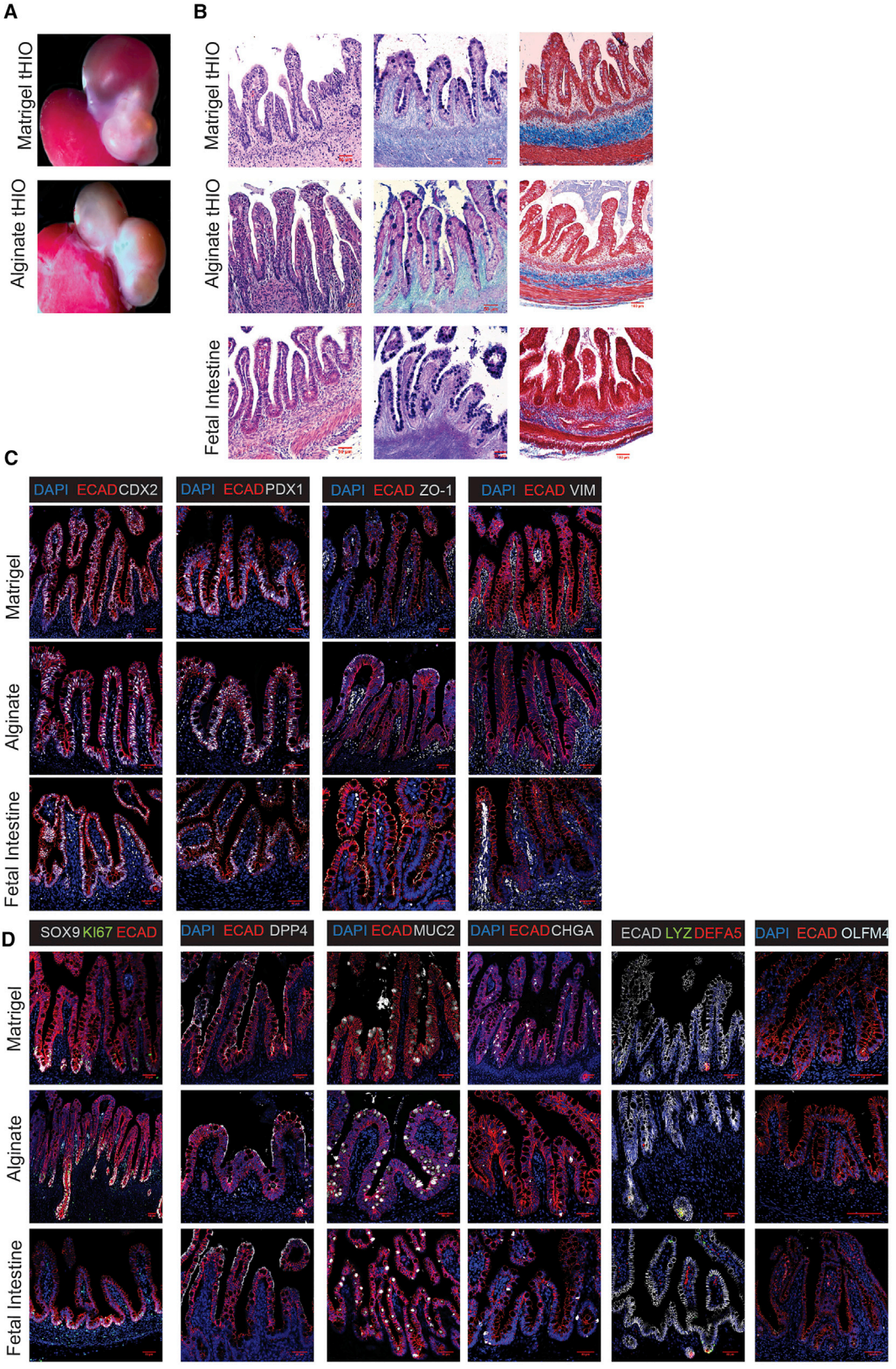

(legend on next page)

supported the development of an outer mesenchyme as evidenced by the presence of VIM expression surrounding the epithelium.

SOX9 is expressed in progenitor cells in HIOs (Hill et al., 2017), and we observed that the majority of epithelial cells in both alginate and Matrigel-grown HIOs expressed SOX9 after 28 days of culture *in vitro*. Co-staining with the proliferation marker KI67 indicated that both alginate and Matrigel-grown HIOs are proliferative (Figure 2C). In addition, both alginate and Matrigel-grown HIOs gave rise to differentiated epithelial cell types *in vitro* as HIOs cultured in the two matrices displayed epithelial cells expressing markers for small intestinal enterocytes (DPP4), goblet cells (MUC2), and enteroendocrine cells (CHGA). This suggests that differentiation within alginate-grown HIOs develops along a similar timeline when compared with Matrigel-grown HIOs.

Although we observed differentiated cell markers within HIOs, the abundance of differentiation was generally low. To report the frequency of differentiation, stemness, and proliferation across multiple HIOs and across different batches of HIOs, we quantified the percentage of HIOs expressing the markers DPP4, MUC2, CHGA, LYZ, DEFA5, VIL1, ZO-1, CDX2, OLFM4, and KI67 across three independent experiments (Figure 2D). Our results demonstrated that alginate and Matrigel-grown HIOs expressed all markers with a similar frequency; however, we noted variability across batches of HIOs. Our data suggest that batch-to-batch variability is the most likely explanation for expression differences between experiments, and this batch effect is seen in alginate and Matrigel-grown HIOs. We also carried out qRT-PCR analysis to compare HIOs from multiple cell lines and further confirmed that alginate or Matrigel-grown HIOs express key epithelial markers at similar levels between growth matrices and across human embryonic stem cell (hESC) or human induced pluripotent stem cell lines (Figure S1D). Taken together, these results demonstrate that alginate-grown HIOs resemble Matrigel-grown HIOs and suggest that alginate is an effective alternative to Matrigel for supporting HIO development *in vitro*.

Transplanted Alginate HIOs Mature *In Vivo*

We next explored the engraftment and maturation potential of alginate-grown HIOs *in vivo*. Matrigel-grown HIOs and HIOs cultured in synthetic matrices have been shown to develop into more mature intestinal tissue after transplantation into immunocompromised (NSG) mice (Cruz-Acuna et al., 2017; Finkbeiner et al., 2015a, 2015b; Watson et al., 2014), so a key success criterion of alginate HIOs is the ability to undergo similar maturation following transplantation into NSG mice. HIOs grown in both 2% alginate (n = 12 mice) and Matrigel (n = 11 mice) were dissociated from their growth matrices and implanted beneath the kidney capsules of NSG mice (Figure 3A). After 10 weeks *in vivo*, transplanted HIOs (tHIOs) previously cultured in alginate developed crypt-villus structures with associated submucosa, lamina propria, and muscularis mucosae resulting in a comparable architecture to tHIOs previously cultured in Matrigel (H&E staining). Both alginate and Matrigel tHIOs displayed goblet cells throughout the villi (Alcian blue/periodic acid–Schiff [PAS] staining) as well as organized collagen fibers in the submucosa (Trichrome staining) (Figure 3B). The structure and features of alginate and Matrigel tHIOs both closely resembled human fetal intestinal tissue (Figure 3B). The epithelium of alginate tHIOs demonstrated evidence that they retained intestinal lineage identity (CDX2+) and remained patterned into duodenum (PDX1+) following transplantation (Figure 3C). Alginate and Matrigel tHIOs both formed ZO-1+ tight junctions at the apical surface of the epithelium, similar to fetal intestinal tissue. In addition, both alginate and Matrigel tHIOs demonstrated the expected localization of mesenchyme inside and below villi as demonstrated by VIM staining.

After growth *in vivo*, alginate tHIOs increased in maturity as evidenced by lack of expression of SOX9 throughout the villi and increased expression of markers for differentiated cell types (Figure 3D). Both SOX9 and KI67 became localized to the crypt-like domains of alginate and Matrigel tHIOs as expected, suggesting the development of a mature crypt-villus axis with proliferative progenitor cells residing

Figure 3. Alginate-Grown HIOs Mature in a Similar Manner as Matrigel-Grown HIOs *In Vivo*

(A) Dissected kidneys containing tHIOs cultured in alginate or Matrigel. HIOs were cultured in either Matrigel or 2% alginate dissolved in H_2O and transplanted after 28 days of culture *in vitro*. tHIOs were removed after 10 weeks *in vivo*.

(B) H&E, Alcian blue/PAS, and Trichrome staining reveal the presence of mature crypt-villus structures in alginate and Matrigel tHIOs. Scale bar, 50 μm (H&E and Alcian blue/PAS), Scale bar, 100 μm Trichrome.

(C) Representative images of general epithelial marker staining in tHIOs from alginate and Matrigel. Markers shown are ECAD (epithelial marker), CDX2 (intestinal epithelium marker), PDX1 (duodenum marker), and VIM (mesenchymal marker). Scale bar, 50 μm.

(D) Representative images of specific epithelial cell marker staining in tHIOs from alginate and Matrigel. Markers shown are SOX9 (progenitor cell marker), KI67 (proliferative cell marker), DPP4 (small intestinal brush border enzyme marker), MUC2 (goblet cell marker), CHGA (enteroendocrine cell marker), LYZ and DEFA5 (Paneth cell markers), and OLFM4 (intestinal stem cell marker). Two transplant experiments were conducted with a total of n = 11 Matrigel transplanted and n = 12 alginate transplanted mice. Scale bar, 50 μm for all markers except OLFM4 scale bar, 100 μm.

in the crypts. The proper localization of intestinal stem cells to the crypts in both alginate and Matrigel tHIOs was confirmed by OLFM4 expression (Dame et al., 2018). Alginate and Matrigel tHIOs similarly expressed DPP4, MUC2, and CHGA throughout the epithelium. In addition, both alginate and Matrigel tHIOs supported the differentiation of Paneth cells localized to crypts as evidenced by co-expression of LYZ and DEFA5, consistent with previous reports (Finkbeiner et al., 2015b; Watson et al., 2014). Staining patterns in alginate and Matrigel tHIOs for all markers closely resembled staining patterns in human fetal intestine. Taken together, these results demonstrate that HIOs grown in alginate differentiate and mature *in vivo* to a similar degree as Matrigel-grown HIOs and highlights alginate as a viable alternative to Matrigel for HIO culture.

The Epithelium of Alginate and Matrigel-Grown HIOs Share a High Degree of Molecular Similarity *In Vitro* and *In Vivo*

We utilized RNA-sequencing analysis to determine the degree of similarity or difference between alginate and Matrigel-grown HIO epithelia in an unbiased manner. In order to reduce variance across samples and specifically assess epithelial gene expression, we isolated the epithelium from alginate and Matrigel-grown HIOs and tHIOs, further expanded this epithelium in identical culture conditions, and then performed bulk RNA-sequencing (Figure 4A). The epithelium from *in vitro* grown HIOs was isolated to create alginate and Matrigel HIO-derived epithelium-only (HdE) cultures. After 10 weeks *in vivo*, the epithelium from alginate and Matrigel tHIOs was similarly isolated and cultured *in vitro* to create alginate and Matrigel transplanted HIO-derived epithelium (tHdE) (Figure 4A). Following RNA-sequencing, the transcriptomic data for individual replicates from all four groups were analyzed for their similarity using Pearson's correlation. Alginate and Matrigel HdEs clustered together with high correlation, and similarly alginate and Matrigel tHdEs formed a cluster with high correlation. These clusters suggest that differences between culture conditions (*in vitro* versus transplantation) are the main drivers of variability between samples as enteroids from *in vitro* grown alginate and Matrigel HIOs are more similar to each other than they are to their transplant-derived counterparts even when grown in uniform culture conditions. This is consistent with previous data showing that HIOs grown *in vitro* are immature/fetal in nature, and transplanted HIOs become more mature/adult-like (Hill et al., 2017).

In addition, we used differential expression analysis to compare alginate and Matrigel HdEs and tHdEs (Figure 4C). There was a high degree of similarity between alginate HdEs (aHdEs) and Matrigel HdEs (mHdEs) with only 32 genes (2.3%) showing significant differences in expression. Similarly, there was high similarity between alginate transplant-derived HdEs (atHdEs) and Matrigel transplant-derived HdEs (mtHdEs) with only 42 genes (3%) displaying significant differences in expression. In contrast, comparison of aHdEs with atHdEs and mHdEs with mtHdEs revealed 730 (51.7%) and 908 (64.4%) genes, respectively, with significant differences in expression. This analysis confirms that the epithelium of alginate HIOs is nearly identical to Matrigel HIOs both *in vitro* and *in vivo*. Genes that are significantly changed in all comparison groups are presented in Table S1.

Alginate Does Not Support Expansion of Epithelium-Only Enteroids

To further test the hypothesis that mesenchyme is critical in forming a niche to support epithelial growth in alginate, and to assess whether alginate can be applied to culture primary human epithelial-only organoids (enteroids), we established primary human fetal enteroid cultures in Matrigel and tested if we could transfer enteroids into alginate. For our experiments, intact small enteroid cysts were manually removed from Matrigel and re-embedded in 1% alginate or Matrigel (Figure S2). Epithelial cysts were viable when transferred into alginate; however, alginate did not support the growth of enteroids while enteroids expanded robustly in Matrigel (Figure S2A). Staining for the basement membrane protein Laminin revealed that the epithelium of enteroids grown in unmodified alginate laid down a basement membrane in an inside-out formation compared with enteroids in Matrigel. That is, Laminin was deposited on the inside of the cyst lumen whereas Laminin surrounded the outside of the epithelial cysts in Matrigel (Figure S2B). This suggests that intestinal epithelial cells are able to lay down a basement membrane in the absence of mesenchymal cells and in the absence of an exogenous ECM (i.e., Matrigel), but that epithelial polarization is altered in this context. There were almost no proliferative epithelial cells observed in enteroids grown in alginate. In contrast, enteroids grown in Matrigel were highly proliferative as assessed by staining for KI67 (Figure S2C). Thus, unmodified alginate does not provide a sufficient niche to support intestinal epithelial proliferation. To investigate whether mesenchymal cells are necessary to promote a niche in a bioinert environment, we cultured intestinal enteroids in the presence of mesenchymal cells isolated from the human fetal intestine. Using a hanging drop co-culture system to generate enteroid-mesenchyme aggregates, we co-cultured enteroids plus intestinal mesenchyme in Matrigel or alginate. In contrast to epithelium-only enteroids grown in alginate, epithelium-mesenchyme aggregates exhibited increased growth and proliferation in alginate (Figures S2A and S2C). Notably, however, epithelium-mesenchyme aggregates grown in alginate still

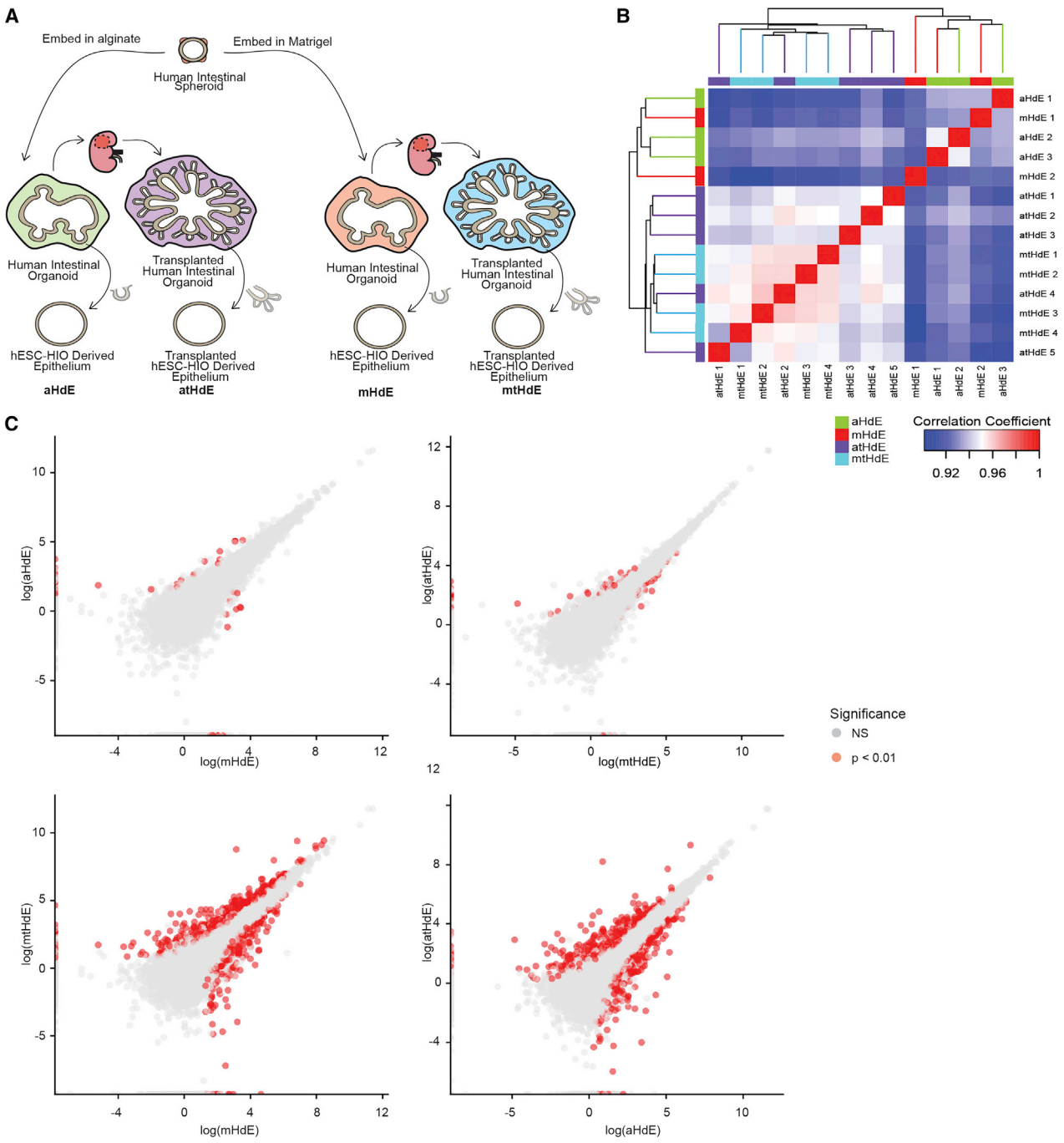

Figure 4. RNA-Sequencing Comparison of Alginate and Matrigel-Grown HIO Epithelia

(A) Schematic overview of sample groups included in RNA-sequencing analysis. Epithelia were extracted from alginate and Matrigel-grown HIOs both after culture *in vitro* and after transplantation into mice.

(B) Clustering HdEs and tHdEs by sample similarity using Pearson's correlation coefficient (n = 3 aHdE, n = 2 mHdE, n = 5 atHdE, n = 4 mtHdE). Clusters formed between aHdEs and mHdEs as well as between atHdEs and mtHdEs.

(C) Differential expression analysis comparing aHdEs with mHdEs, atHdEs with mtHdEs, mHdEs with mtHdEs, and aHdEs with atHdEs. Red dots represent genes with significant differences in expression ($p < 0.01$). In these plots, the alginate and Matrigel samples are nearly identical. RNA-sequencing data have been deposited in the ArrayExpress database at EMBL-EBI (www.ebi.ac.uk/arrayexpress) under accession number ArrayExpress: E-MTAB-7000.

See also Table S1.

remained inside-out with the mesenchyme restricted to the inside of the cysts, and with the apical surface facing outwards. This suggests that the presence of mesenchyme is sufficient to at least partially establish an epithelial niche that promotes epithelial proliferation in alginate and provides evidence that primary epithelium-only enteroid cultures do not grow in unmodified alginate in a manner that is comparable to Matrigel.

DISCUSSION

In this work we identified alginate as a minimally supportive growth matrix that supports HIO development both *in vitro* and *in vivo*. We showed that HIO survival is dependent on alginate polymer density, with concentrations of 1% to 2% alginate (w/v) selected to best support viability at early time points as well as maximize overall HIO yield. The mechanical properties of alginate and PEG hydrogels optimized for HIO formation were similar, confirming the reliance of HIO viability on matrix stiffness (Cruz-Acuna et al., 2017). While alginate supported HIO survival *in vitro*, the resulting yields after 28 days were significantly lower than yields in Matrigel. However, the yields we observed in 1% and 2% alginate are comparable with yields previously reported for HIOs cultured in Matrigel, and could likely be optimized by sorting spheroids for size or characteristic to improve yield (Arora et al., 2017). Further, alginate-grown HIOs can be passaged and maintained for at least 90 days *in vitro* without significant decreases in expression of key markers (Figure S3A), further demonstrating the utility of alginate as a replacement to Matrigel.

It is unclear whether alginate results in lower overall yield of HIOs as compared with previously described synthetic polymers since viability was only reported at early time points in previous work (Cruz-Acuna et al., 2017). Lower HIO yields in alginate as compared to Matrigel may be due to the inability of cells to remodel the hydrogel, lack of interactions with serum proteins, or the lack of growth factors present in Matrigel. A comparison of HIO yield in four-arm polyethylene glycol with maleimide groups at each terminus (PEG-4MAL) modified with the adhesive peptide RGD and crosslinked with the protease degradable peptide GPQ-W as previously described (Cruz-Acuna et al., 2017, 2018) did not provide conclusive evidence on whether decreased yields in alginate may be due to lack of adhesive or degradable cues (Figure S3B). To further resolve ways in which matrix properties affect HIO characteristics, future work should investigate longer-term studies with a larger sample size and include alginates modified with adhesive/degradable peptides to compare results within a single hydrogel system rather than introducing variability across hydrogels by utilizing PEG-4MAL.

HIOs cultured in alginate resulted in tissue indistinguishable from Matrigel-grown HIOs at the epithelial level. Importantly, both matrices supported further differentiation and maturation *in vivo*, illustrating that HIOs cultured in alginate retain the potential to develop into mature intestinal tissue that resembles human fetal intestine. While the epithelia from alginate and Matrigel-grown HIOs were highly similar, it remains unclear whether or not there are differences at the mesenchymal level. It is interesting to note that the mesenchyme of alginate-grown HIOs did not invade the surrounding matrix as in Matrigel-grown HIOs. Further research is necessary to elucidate potential mesenchymal differences between alginate and Matrigel-grown HIOs.

Given the similarities between alginate and Matrigel-grown HIOs, alginate is an effective alternative to Matrigel-based culture systems, which eliminates reliance on animal-derived materials and reduces cost, thereby increasing translational potential. The alginate used in our experiments cost approximately 320 times less than PEG and 700–900 times less than Matrigel (~$0.44 alginate versus ~$140 PEG versus ~$300-$400 Matrigel per 10 mL, depending on type), presenting a critical cost advantage for both basic and translational studies. Of note, PEG-4MAL-grown HIOs need to be passaged and embedded in fresh gels approximately once per week due to degradation of the hydrogel, whereas alginate-grown HIOs can be cultured for up to 30 days without passaging due to the nondegradable nature of alginate, presenting an additional advantage for cost and ease of use.

From a biological standpoint, perhaps the most interesting observation of HIO culture in alginate is that HIOs do not require external cues from the extracellular matrix. The alginate we utilized in this work was not modified with adhesive peptides to support HIO growth and was thus biologically inert, providing purely mechanical support to developing HIOs. The lack of adhesive or biochemical cues from the hydrogel suggests that HIOs are able to create their own niche, likely through the basement membrane and trophic support that is established between the epithelium and mesenchyme. This hypothesis is strengthened by the inability of intestinal epithelium-only enteroids to proliferate in unmodified alginate unless they are co-cultured with mesenchymal cells. The lack of chemical modifications makes alginate a simple system that lends nicely toward large scale production, but the polymer can easily be modified for further research (Augst et al., 2006; Rowley et al., 1999). Future experiments testing alginates modified with adhesive/degradable cues may enable primary enteroid culture in alginate in the absence of mesenchymal cells. However, as a natural matrix, alginate does come with the limitation of batch-to-batch variability as with Matrigel (Fu et al., 2010), but our experiments found that alginate was

able to optimally support growth over a range of conditions, so small variations between batches should not cause a large change in matrix efficacy. The system described here can likely be implemented to support additional 3D culture systems in a simple, cost-effective manner to advance regenerative medicine.

EXPERIMENTAL PROCEDURES

hESC/hiPSC Lines and Generation of hPSC-Derived Intestinal Organoids

Human ES lines H9 and H1 (NIH registry #0062 and #0042) were obtained from the WiCell Research Institute. Rockefeller University Embryonic Stem Cell Line 2 (NIH registry # 0013) Germ Layer Reporter (RUES2-GLR) was obtained as a kind gift from Dr. Ali Brivanlou (Martyn et al., 2018). Human iPSC Line 72.3 was obtained from Cincinnati Children's Hospital Medical Center (McCracken et al., 2015). All experiments using human ES cells were approved by the University of Michigan Human Pluripotent Stem Cell Research Oversight Committee. hPSC lines are routinely karyotyped to ensure normal karyotype and monthly mycoplasma monitoring is conducted on all cell lines using the MycoAlert Mycoplasma Detection Kit (Lonza). H9 cells were authenticated using Short Tandem Repeat (STR) DNA profiling (Matsuo et al., 1999) at the University of Michigan DNA Sequencing Core and exhibited an STR profile identical to the STR characteristics published by Josephson et al. (2006). Stem cell maintenance and generation of hindgut spheroids was performed as described previously (Hill et al., 2017; Spence et al., 2011; Tsai et al., 2017). After differentiation, hindgut spheroids were collected from differentiated stem cell cultures and plated in either Matrigel or alginate droplets on a 24-well tissue culture grade plate and maintained in organoid growth medium. See Supplemental Experimental Procedures for more information.

Epithelial Isolation

Generation of HdEs and tHdEs from HIOs and tHIOs was performed using previously described methods to isolate the epithelium (Tsai et al., 2018). See Supplemental Experimental Procedures for more information.

Human Tissue

Normal, de-identified human fetal intestinal tissue was obtained from the University of Washington Laboratory of Developmental Biology. Tissue sections were obtained from formalin fixed, paraffin-embedded 14- to 15-week fetal intestinal specimens. All research using human tissue was approved by the University of Michigan institutional review board.

Mouse Kidney Capsule Transplantation

The University of Michigan and Cincinnati Children's Hospital Institutional Animal Care and Use Committees approved all animal research. Prior to transplantation, HIOs were mechanically dissociated from either alginate or Matrigel by pipetting up and down and scraping away alginate/Matrigel with a scalpel. HIOs were implanted under the kidney capsules of immunocompromised NOD-SCID IL2Rg-null (NSG) mice (Jackson Laboratory strain no. 0005557) as previously described (Finkbeiner et al., 2015b). In summary, mice were anesthetized using 2% isoflurane. A left-flank incision was used to expose the kidney after shaving and sterilization with isopropyl alcohol. HIOs cultured in alginate and Matrigel were surgically implanted beneath mouse kidney capsules using forceps. Prior to closure, an intraperitoneal flush of Zosyn (100 mg kg^{-1}; Pfizer) was administered. Mice were euthanized for retrieval of tHIOs after 10 weeks. Results shown are representative of two experiments performed with a total of n = 11 mice (Matrigel tHIOs) and n = 12 mice (alginate tHIOs), with at least one organoid implanted per kidney capsule, depending on HIO size.

Alginate Gel Formation

Low-viscosity sodium alginate powder (Alfa Aesar, B25266) was dissolved in 1 mL of 1 × PBS or H_2O to dilutions of 0.5%–4% (w/v). The alginate solution was then heated to 98°C for 30 min on a heating block to improve sterility and ensure that the alginate fully dissolved. Excess alginate solutions were stored at room temperature and used within 1 week of initial preparation. Spheroids were suspended in the alginate solutions at a density of approximately 50 spheroids per 45 μL; 5 μL droplets of 2% (w/v) calcium chloride (Sigma-Aldrich, 449709) were deposited on the bottom of 24-well tissue culture plates (Nunclon), and 45 μL of alginate containing spheroids was then pipetted directly onto the calcium chloride solution to initiate ionic crosslinking, which began instantaneously upon pipetting. Gels were formed one plate at a time to avoid calcium chloride evaporation. The gels polymerized at room temperature for 5–10 min and were then placed into a tissue culture incubator and allowed to fully set for 20 min at 37°C before media was added, replicating the protocol for Matrigel. HIOs cultured in 1% and 2% alginate were used to obtain all data in Figures 2, 3, and 4.

Mechanical Characterization of Alginate Hydrogels

The storage and loss moduli of the alginate gels were determined by performing *in situ* gelation tests on an AR-G2 rheometer equipped with a Peltier stage and 20 mm measurement head. In brief, 90 μL of alginate was deposited onto the bottom of the rheometer while 10 μL of 2% $CaCl_2$ was deposited onto the measurement head. The head was lowered to a gap height of 300 μm initiating gelation upon contact, and then the edges of the gel were sealed with mineral oil. The mechanical response of the gels was recorded by performing time sweep measurements at a constant strain of 6% and a frequency of 1 rad/s. The time sweep was continued until storage and loss moduli reached steady state indicating completion of gelation. Rheological testing of alginate was carried out at room temperature, representing the initial gelation conditions of alginate that polymerizes at room temperature within 5 min prior to storage at 37°C. Matrigel rheology was carried out in the same manner but measurements were obtained at 37°C as Matrigel takes more than 20 min to polymerize and gelation occurs at 37°C.

Viability Assay and Quantification

Alginate gels and Matrigel droplets were incubated in 1 μM Calcein-AM (live; ThermoFisher), and 0.5 μM Ethidium-homodimer (dead; ThermoFisher) in PBS for 30 min. Samples were imaged using an Olympus IX73 Inverted microscope or Nikon A-

1 confocal microscope. Quantification of viability was performed by calculating the percentage of the total projected area of a spheroid/organoid that stained positive for the live or dead stain using ImageJ (National Institutes of Health, USA). The results are representative of three independent experiments performed with $n \geq 6$ gel samples per experimental group.

RNA-Sequencing and Bioinformatics Analysis

RNA isolation and analysis was carried out as previously described (Tsai et al., 2018). See Supplemental Experimental Procedures for more information.

Tissue Preparation, Immunohistochemistry, Electron Microscopy and Imaging

Paraffin Sectioning and Staining

HIO and tHIO tissues were fixed in 4% paraformaldehyde (Sigma) overnight and then dehydrated in an alcohol series: 30 min each in 25%, 50%, 75% Methanol:PBS/0.05% Tween 20, followed by 100% methanol, and then 100% ethanol. Tissue was processed into paraffin using an automated tissue processor (Leica ASP300). Paraffin blocks were sectioned 7-μM thick, and immunohistochemical staining was performed as previously described (Spence et al., 2009). A list of antibody information and concentrations used can be found in the Supplemental Experimental Procedures. H&E staining was performed using Harris Modified Hematoxylin (FisherScientific) and Shandon Eosin Y (ThermoScientific) according to the manufacturer's instructions. Alcian blue/PAS staining was performed using the Newcomer Supply Alcian blue/PAS Stain kit (Newcomer Supply, Inc.) according to manufacturer's instructions. Trichrome staining was performed by the University of Michigan *in vivo* Animal Core.

Imaging and Image Processing

Fluorescently stained slides were imaged on a Nikon A-1 confocal microscope. Brightness and contrast adjustments were carried out using ImageJ (National Institutes of Health) and adjustments were made uniformly across images.

Quantification and Statistical Analysis

Statistical analyses and plots were generated in Prism 6 software (GraphPad). If more than two groups were being compared within a single experiment, an unpaired one-way ANOVA was performed followed by Tukey's multiple comparisons test to compare the mean of each group with the mean of every other group within the experiment unless otherwise specified. For all statistical tests, a significance value of 0.05 was used. For every analysis, the strength of p values is reported in the figures according the following: $p > 0.05$, $*p \leq 0.05$, $**p \leq 0.01$, $***p \leq 0.001$, $****p \leq 0.0001$. Details of statistical tests can be found in the figure legends.

ACCESSION NUMBERS

RNA-seq data have been deposited in the ArrayExpress database at EMBL-EBI under accession number ArrayExpress: E-MTAB-7000.

SUPPLEMENTAL INFORMATION

Supplemental Information includes Supplemental Experimental Procedures, three figures, and one table and can be found with this article online at https://doi.org/10.1016/j.stemcr.2018.12.001.

AUTHOR CONTRIBUTIONS

Project conceptualization: M.M.C., S.H., S.T., and J.R.S. Experimental design: M.M.C., J.R.S., M.C., S.H., Y.S., E.A., M.H., A.J.G., and A.J.P. Experiments and data collection: M.M.C., M.C., S.H., Y.S., Y.-H.T., A.W., B.J., N.S., M.H., and A.J.G. Data analysis and interpretation: M.M.C., M.C., S.H., Y.-H.T., A.W., M.S.N., B.J., N.S., S.T., M.H., A.J.P, and J.R.S. Critical materials: A.J.G. (modified PEG hydrogels). Writing manuscript: M.M.C. and J.R.S. Editing manuscript: all authors.

ACKNOWLEDGMENTS

This work was supported by the Intestinal Stem Cell Consortium (U01DK103141 to J.R.S.), a collaborative research project funded by the National Institute of Diabetes and Digestive and Kidney Diseases (NIDDK) and the National Institute of Allergy and Infectious Diseases (NIAID). This work was also supported by the NIAID Novel Alternative Model Systems for Enteric Diseases (NAMSED) consortium (U19AI116482 to J.R.S. and S.T.). M.M.C. was supported by the Cellular and Biotechnology Training Program NIGMS T32GM008353; M.C. was supported by the Training Program in Organogenesis Fellowship NICHD T32HD007505. The Laboratory of Developmental Biology, University of Washington, Seattle, WA, United States is supported by NICHD R24HD000836 to Ian Glass. The content is solely the responsibility of the authors and does not necessarily represent the official views of the National Institutes of Health.

Received: July 8, 2018
Revised: December 2, 2018
Accepted: December 5, 2018
Published: January 3, 2019

REFERENCES

Arora, N., Alsous, J.I., Guggenheim, J.W., Mak, M., Munera, J., Wells, J.M., Kamm, R.D., Asada, H.H., Shvartsman, S.Y., and Griffith, L.G. (2017). A process engineering approach to increase organoid yield. Development *144*, 1128–1136.

Augst, A.D., Kong, H.J., and Mooney, D.J. (2006). Alginate hydrogels as biomaterials. Macromol. Biosci. *6*, 623–633.

Aurora, M., and Spence, J.R. (2016). hPSC-derived lung and intestinal organoids as models of human fetal tissue. Dev. Biol. *420*, 230–238.

Chaudhuri, O. (2017). Viscoelastic hydrogels for 3D cell culture. Biomater. Sci. *5*, 1480–1490.

Cruz-Acuna, R., Quiros, M., Farkas, A.E., Dedhia, P.H., Huang, S., Siuda, D., Garcia-Hernandez, V., Miller, A.J., Spence, J.R., Nusrat, A., and Garcia, A.J. (2017). Synthetic hydrogels for human intestinal organoid generation and colonic wound repair. Nat. Cell Biol. *19*, 1326–1335.

Cruz-Acuna, R., Quiros, M., Huang, S., Siuda, D., Spence, J.R., Nusrat, A., and Garcia, A.J. (2018). PEG-4MAL hydrogels for human organoid generation, culture, and in vivo delivery. Nat. Protoc. *13*, 2102–2119.

Czerwinski, M., and Spence, J.R. (2017). Hacking the matrix. Cell Stem Cell *20*, 9–10.

Dame, M., Attili, D., McClintock, S., Dedhia, P.H., Ouillette, P., Hardt, O., Chin, A.M., Xue, X., Laliberte, J., Katz, E., et al. (2018). Identification, isolation and characterization of human LGR5-positive colon adenoma cells. Development *145*, dev153409.

Dedhia, P.H., Bertaux-Skeirik, N., Zavros, Y., and Spence, J.R. (2016). Organoid models of human gastrointestinal development and disease. Gastroenterology *150*, 1098–1112.

Dye, B., Dedhia, P.H., Miller, A.J., Nagy, M.S., White, E.S., Shea, L., and Spence, J.R. (2016). A bioengineered niche promotes in vivo engraftment and maturation of pluripotent stem cell derived human lung organoids. Elife *5*. https://doi.org/10.7554/eLife.19732.

Dye, B., Hill, D.R., Ferguson, M., Tsai, Y.-H., Nagy, M.S., Dyal, R., Wells, J.M., Mayhew, C.N., Nattiv, R., Klein, O.D., et al. (2015). In vitro generation of human pluripotent stem cell derived lung organoids. Elife *4*. https://doi.org/10.7554/eLife.05098.

Eiraku, M., Takata, N., Kawada, M., Sakakura, E., Okuda, S., Sekiguchi, K., Adachi, T., and Sasai, Y. (2011). Self-organizing optic-cup morphogenesis in three-dimensional culture. Nature *472*, 51–56.

Enemchukwu, N.O., Cruz-Acuna, R., Bongiorno, T., Johnson, C.T., Garcia, J.R., Sulchek, T., and Garcia, A.J. (2016). Synthetic matrices reveal contributions of ECM biophysical and biochemical properties to epithelial morphogenesis. J. Cell Biol. *212*, 113–124.

Finkbeiner, S.R., Freeman, J.J., Wieck, M.M., El-Nachef, W., Altheim, C.H., Tsai, Y.-H., Huang, S., Dyal, R., White, E.S., Grikscheit, T.C., et al. (2015a). Generation of tissue-engineered small intestine using embryonic stem cell-derived human intestinal organoids. Biol. Open *4*, 1462–1472.

Finkbeiner, S.R., Hill, D.R., Altheim, C.H., Dedhia, P.H., Taylor, M.J., Tsai, Y.-H., Chin, A.M., Mahe, M.M., Watson, C.L., Freeman, J.J., et al. (2015b). Transcriptome-wide analysis reveals hallmarks of human intestine development and maturation in vitro and in vivo. Stem Cell Reports *4*, 1140–1155.

Forgacs, G., Foty, R.A., Shafrir, Y., and Steinberg, M.S. (1998). Viscoelastic properties of living embryonic tissue: a quantitative study. Biophys. J. *74*, 2227–2234.

Fu, S., Thacker, A., Sperger, D.M., Boni, R.L., Valankar, S., Munson, E.J., and Block, L.H. (2010). Rheological evaluation of inter-grade and inter-batch variability of sodium alginate. AAPS PharmSciTech *11*, 1662–1674.

Gjorevski, N., Sachs, N., Manfrin, A., Giger, S., Bragina, M.E., Ordonez-Moran, P., Clevers, H., and Lutolf, M.P. (2016). Designer matrices for intestinal stem cell and organoid culture. Nature *539*, 560–564.

Hill, D.R., Huang, S., Nagy, M.S., Yadagiri, V.K., Fields, C., Muckherjee, D., Bons, B., Dedhia, P.H., Chin, A.M., Tsai, Y.-H., et al. (2017). Bacterial colonization stimulates a complex physiological response in the immature human intestinal epithelium. Elife *6*. https://doi.org/10.7554/eLife.29132.

Huch, M., Knoblich, J.A., Lutolf, M.P., and Martinez-Arias, A. (2017). The hope and hype of organoid research. Development *144*, 938–941.

Jeon, O., Alt, D.S., Linderman, S.W., and Alsberg, E. (2013). Biochemical and physical signal gradients in hydrogels to control stem cell behavior. Adv. Mater. *25*, 6366–6372.

Johnston, D.S. (2015). The renaissance of developmental biology. PLoS Biol. *13*, e1002149.

Josephson, R., Sykes, G., Liu, Y., Ording, C., Xu, W., Zeng, X., Shin, S., Loring, J., Maitra, A., Rao, M.S., and Auerbach, J.M. (2006). A molecular scheme for improved characterization of human embryonic stem cell lines. BMC Biol. *4*, 28.

Lancaster, M., Renner, M., Martin, C., Wenzel, D., Bicknell, L., Hurles, M., Homfay, T., Penninger, J., Jackson, A., and Knoblich, J. (2013). Cerebral organoids model human brain development and microcephaly. Nature *501*, 373–379.

Lee, K.Y., and Mooney, D.J. (2012). Alginate: properties and biomedical applications. Prog. Polym. Sci. *37*, 106–126.

Little, M.H. (2017). Organoids: a special issue. Development *144*, 935–937.

Martyn, I., Kanno, T.Y., Ruzo, A., Siggia, E.D., and Brivanlou, A.H. (2018). Self-organization of a human organizer by combined Wnt and nodal signalling. Nature *558*, 132–135.

Matsuo, Y., Nishizaki, C., and Drexler, H.G. (1999). Efficient DNA fingerprinting method for the identification of cross-culture contamination of cell lines. Human Cell *12*, 149–154.

McCracken, K., Cata, E.M., Crawford, C.M., Sinagoga, K.L., Schumacher, M., Rockich, B.E., Tsai, Y.-H., Mayhew, C.N., Spence, J.R., Zavros, Y., and Wells, J.M. (2015). Modeling human development and disease in pluripotent stem cell-derived gastric organoids. Nature *516*, 400–404.

McCracken, K., Howell, J., Wells, J.M., and Spence, J.R. (2011). Generating human intestinal tissue from pluripotent stem cells in vitro. Nat. Protoc. *6*, 1920–1928.

Miller, A.J., Hill, D.R., Nagy, M.S., Aoki, Y., Dye, B., Chin, A.M., Huang, S., Zhu, F., White, E.S., Lama, V., and Spence, J.R. (2018). In vitro induction and in vivo engraftment of lung bud tip progenitor cells derived from human pluripotent stem cells. Stem Cell Reports *10*, 101–119.

Munera, J., Sundaram, N., Rankin, S., Hill, D., Watson, C., Mahe, M., Vallance, J., Shroyer, N., Sinagoga, K., Zarzoso-Lacoste, A., et al. (2017). Differentiation of human pluripotent stem cells into colonic organoids via transient activation of BMP signaling. Cell Stem Cell *21*, 51–64.

Rowley, J.A., Madlambayan, G., and Mooney, D.J. (1999). Alginate hydrogels as synthetic extracellular matrix materials. Biomaterials *20*, 45–53.

Samorezov, J.E., Morlock, C.M., and Alsberg, E. (2015). Dual ionic and photo-crosslinked alginate hydrogels for micropatterned spatial control of material properties and cell behavior. Bioconjug. Chem. *26*, 1339–1347.

Singagoga, K.L., and Wells, J.M. (2015). Generating human intestinal tissues from pluripotent stem cells to study development and disease. EMBO J. *34*, 1149–1163.

Spence, J.R., Lange, A.W., Lin, S.-C.J., Kaestner, K.H., Lowy, A.M., Kim, I., Whitsett, J.A., and Wells, J.M. (2009). Sox17 regulates organ lineage segregation of ventral foregut progenitor cells. Dev. Cell *17*, 62–74.

Spence, J.R., Mayhew, C.N., Rankin, S.A., Kuhar, M., Vallance, J.E., Tolle, K., Hoskins, E.E., Kalinichenko, V.V., Wells, S.I., Zorn, A.M., et al. (2011). Directed differentiation of human pluripotent stem cells into intestinal tissue in vitro. Nature *470*, 105–109.

Takasato, M., Er, P.X., Becroft, M., Vanslambrouck, J.M., Stanley, E.G., Elefanty, A.G., and Little, M.H. (2014). Directing human embryonic stem cell differentiation towards a renal-lineage generates a self-organizing kidney. Nat. Cell Biol. *16*, 118–126.

Takebe, T., Sekine, K., Enomura, M., Koike, H., Kimura, M., Ogaeri, T., Zhang, R.-R., Ueno, Y., Zheng, Y.-W., Koike, N., et al. (2013). Vascularized and functional human liver from an iPSC-derived organ bud transplant. Nature *499*, 481–484.

Tsai, Y.-H., Czerwinski, M., Wu, A., Dame, M., Attili, D., Hill, E., Colacino, J., Nowacki, L.M., Shroyer, N., Higgins, P.D., et al. (2018). A method for cryogenic preservation of human biopsies and subsequent organoid culture. Cell. Mol. Gastroenterol. Hepatol. *6*, 218–222.e7.

Tsai, Y.-H., Hill, D.R., Kumar, N., Huang, S., Chin, A.M., Dye, B., Nagy, M.S., Verzi, M., and Spence, J.R. (2016). LGR4 and LGR5 function redundantly during human endoderm differentiation. Cell. Mol. Gastroenterol. Hepatol. *2*, 648–662.

Tsai, Y.-H., Nattiv, R., Dedhia, P.H., Nagy, M.S., Chin, A.M., Thomson, M., Klein, O.D., and Spence, J.R. (2017). In vitro patterning of pluripotent stem cell-derived intestine recapitulates in vivo human development. Development *144*, 1045–1055.

Watson, C., Mahe, M., Junera, J., Howell, J., Sundaram, N., Poling, H., Schweitzer, J., Vallance, J., Mayhew, C., Sun, Y., et al. (2014). An in vivo model of human small intestine using pluripotent stem cells. Nat. Med. *2014*, 1310–1314.

Webber, R.E., and Shull, K.R. (2004). Strain dependence of the viscoelastic properties of alginate hydrogels. Macromolecules *37*, 6153–6160.

Wells, J.M., and Spence, J.R. (2014). How to make an intestine. Development *141*, 752–760.

Stem Cell Reports, Volume *12*

Supplemental Information

Nonadhesive Alginate Hydrogels Support Growth of Pluripotent Stem Cell-Derived Intestinal Organoids

Meghan M. Capeling, Michael Czerwinski, Sha Huang, Yu-Hwai Tsai, Angeline Wu, Melinda S. Nagy, Benjamin Juliar, Nambirajan Sundaram, Yang Song, Woojin M. Han, Shuichi Takayama, Eben Alsberg, Andres J. Garcia, Michael Helmrath, Andrew J. Putnam, and Jason R. Spence

Inventory of Supplemental Information:

Figure S1. Alginate supports HIO culture across multiple hPSC lines. This Figure is related to Figures 1 and 2 as we present evidence that HIOs derived from multiple hPSC lines can be cultured in alginate and present qRT-PCR analysis to compare expression levels of key epithelial genes between alginate and Matrigel-grown HIOs across multiple hPSC lines.

Figure S2. Alginate does not recapitulate intestinal epithelial niche in the absence of mesenchymal support. This Figure is related to Figures 1 and 2 as we demonstrate that organoid culture in alginate cannot be expanded to primary intestinal enteroids that lack a mesenchymal component, and provide preliminary evidence suggesting that mesenchymal support creates a niche to support intestinal epithelium in alginate.

Figure S3. Further characterization of alginate-grown HIOs. This Figure is related to Figure 1 as we demonstrate that HIO culture in alginate can be continued for up to 90 days.

Table S1. This Table is related to Figure 4 as we provide an Excel file listing specific genes that are significantly changed in all comparison groups in Figure 4.

Supplemental Experimental Procedures

- **Expanded methods**
- **qRT-PCR primer sequences**
- **Antibody information**

Supplemental References

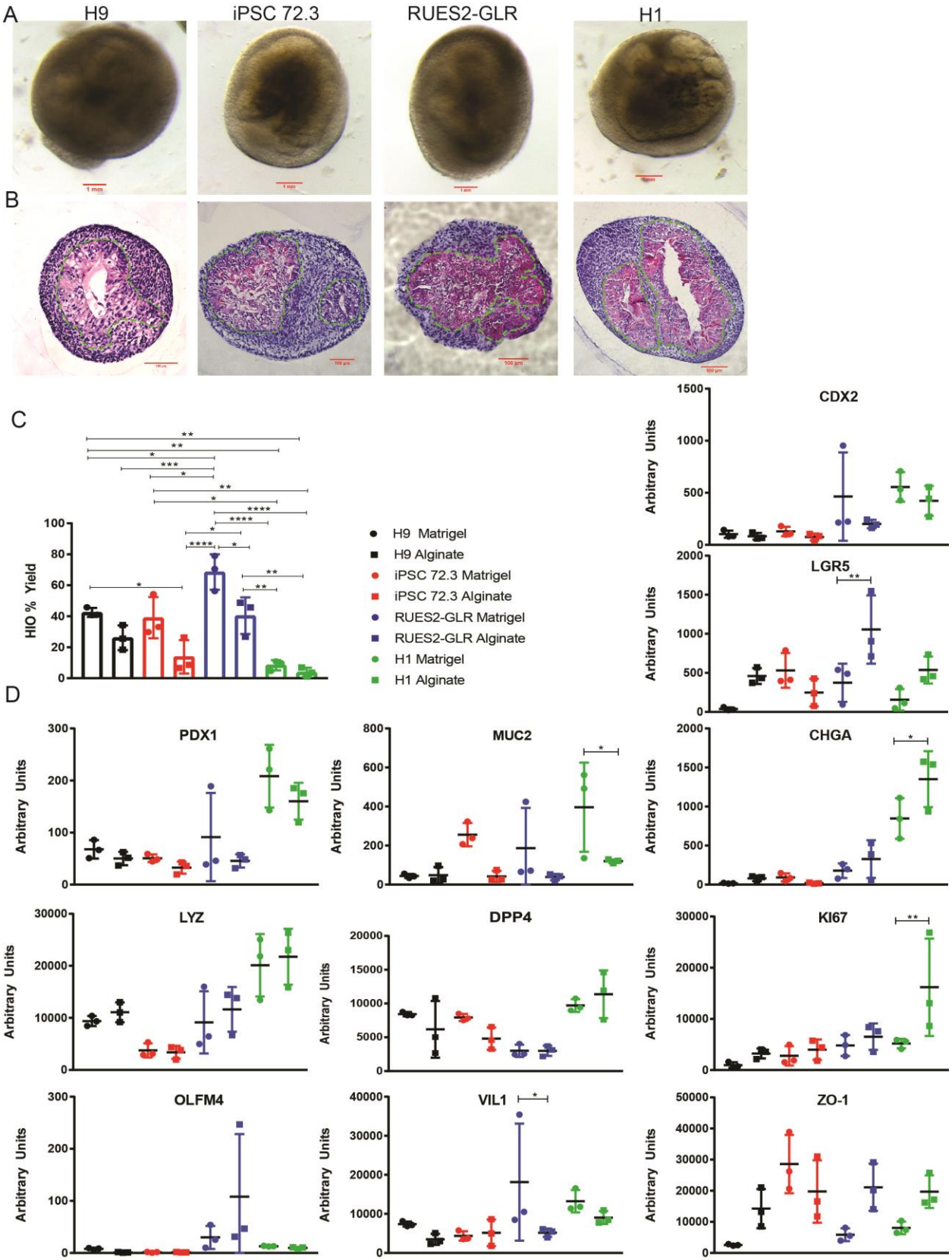
A
H9
iPSC 72.3
RUES2-GLR
H1
B
C
HIO % Yield
H9 Matrigel
H9 Alginate
iPSC 72.3 Matrigel
iPSC 72.3 Alginate
RUES2-GLR Matrigel
RUES2-GLR Alginate
H1 Matrigel
H1 Alginate
CDX2
LGR5
D
PDX1
MUC2
CHGA
LYZ
DPP4
KI67
OLFM4
VIL1
ZO-1
Arbitrary Units

Figure S1. Alginate supports HIO culture across multiple hPSC lines. Related to Figures 1 and 2. **(a)**: Brightfield images of HIOs derived from 4 independent hPSC lines cultured in 1% alginate for 28 days *in vitro*. Scale bar, 1 mm. **(b):** Hematoxylin and eosin (H&E) staining of HIOs derived from 4 independent hPSC lines cultured in 1% alginate for 28 days. Dashed lines outline the epithelium. Scale bar, 100μm. **(c)**: Quantification of HIO yield after 28 days in culture for HIOs derived from 4 independent hPSC lines. HIO yield was calculated as the percentage of spheroids which gave rise to HIOs. Data shown are the average yields from 3 independent experiments with n>100 spheroids per condition. Each point depicts overall yield from one experiment, while bars depict mean and SE. Significance was calculated with a one-way ANOVA and Tukey's multiple comparisons test. The strength of p values is reported according the following: $p > 0.05$, $*p \leq 0.05$, $**p \leq 0.01$, $***p \leq 0.001$, $****p \leq 0.0001$. **(d)**: qRT-PCR analysis of CDX2, LGR5, PDX1, MUC2, CHGA, LYZ, DPP4, KI67, OLFM4, VIL1, ZO-1 expression in HIOs derived from 4 independent hPSC lines cultured in 1% alginate and Matrigel for 28 days *in vitro*. Expression levels are normalized to ECAD expression to account for varying amounts of epithelium in HIOs. Each point is representative of 6-10 HIOs pooled from the same batch. Data represent the mean ± SE. Significance was calculated with a one-way ANOVA and Tukey's multiple comparisons test where expression was compared between alginate and Matrigel-grown HIOs for each line. The strength of p values is reported according the following: $p > 0.05$, $*p \leq 0.05$, $**p \leq 0.01$, $***p \leq 0.001$, $****p \leq 0.0001$.

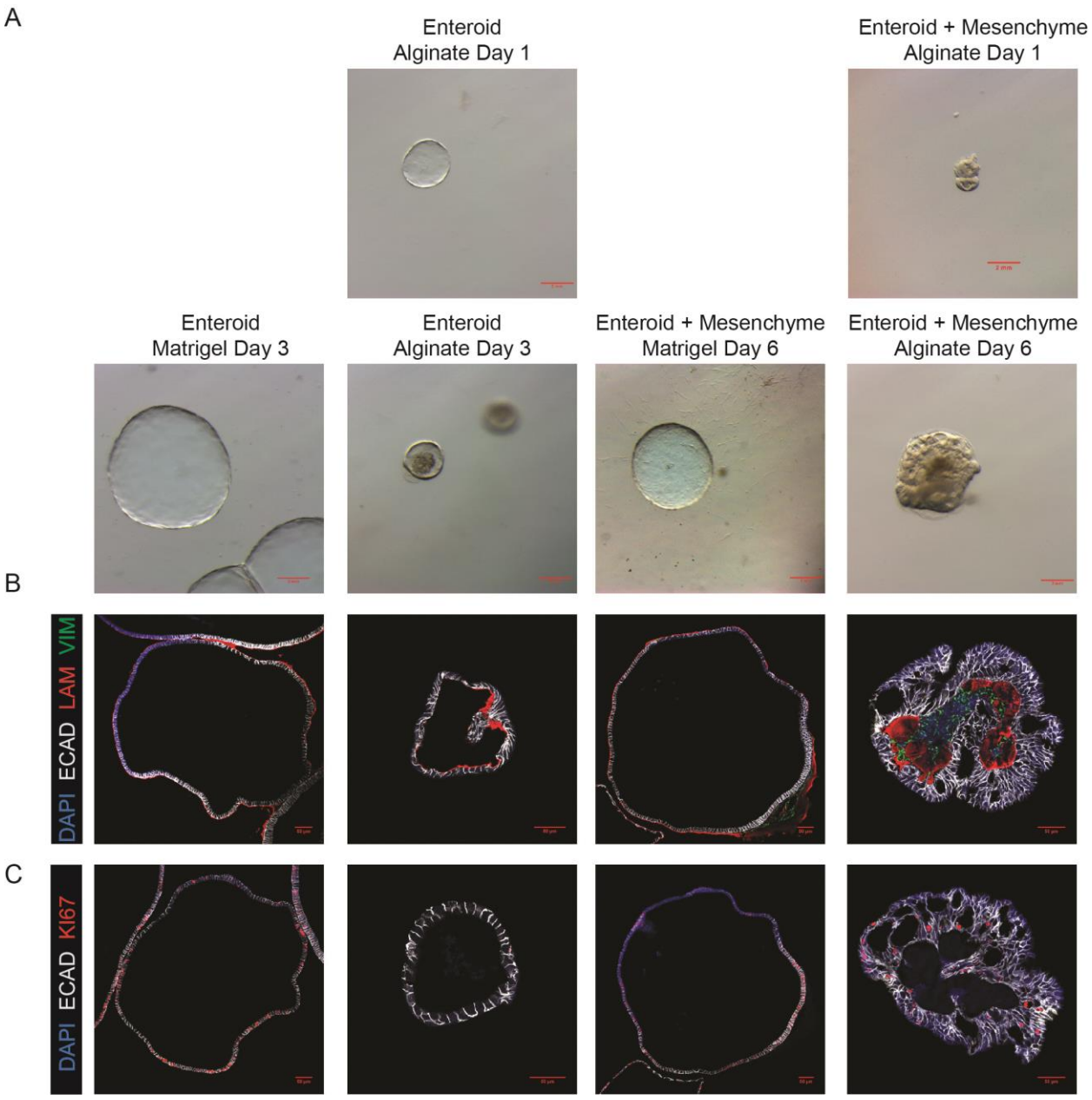

Figure S2. Alginate does not recapitulate intestinal epithelial niche in the absence of mesenchymal support. Related to Figures 1 and 2. **(a)**: Brightfield images of fetal intestinal enteroids cultured in Matrigel and re-embed in 1% alginate and Matrigel either alone or co-cultured with fetal intestinal mesenchymal cells. Scale bar, 1 mm. **(b)**: Representative images of intestinal enteroids embed in alginate and Matrigel with and without mesenchyme after 7 days stained for ECAD, LAM, and VIM. Scale bar, 50 µm. **(c)**: Representative images of intestinal enteroids embed in alginate and Matrigel with and without mesenchyme after 7 days stained for ECAD and KI67. Scale bar, 50 µm.

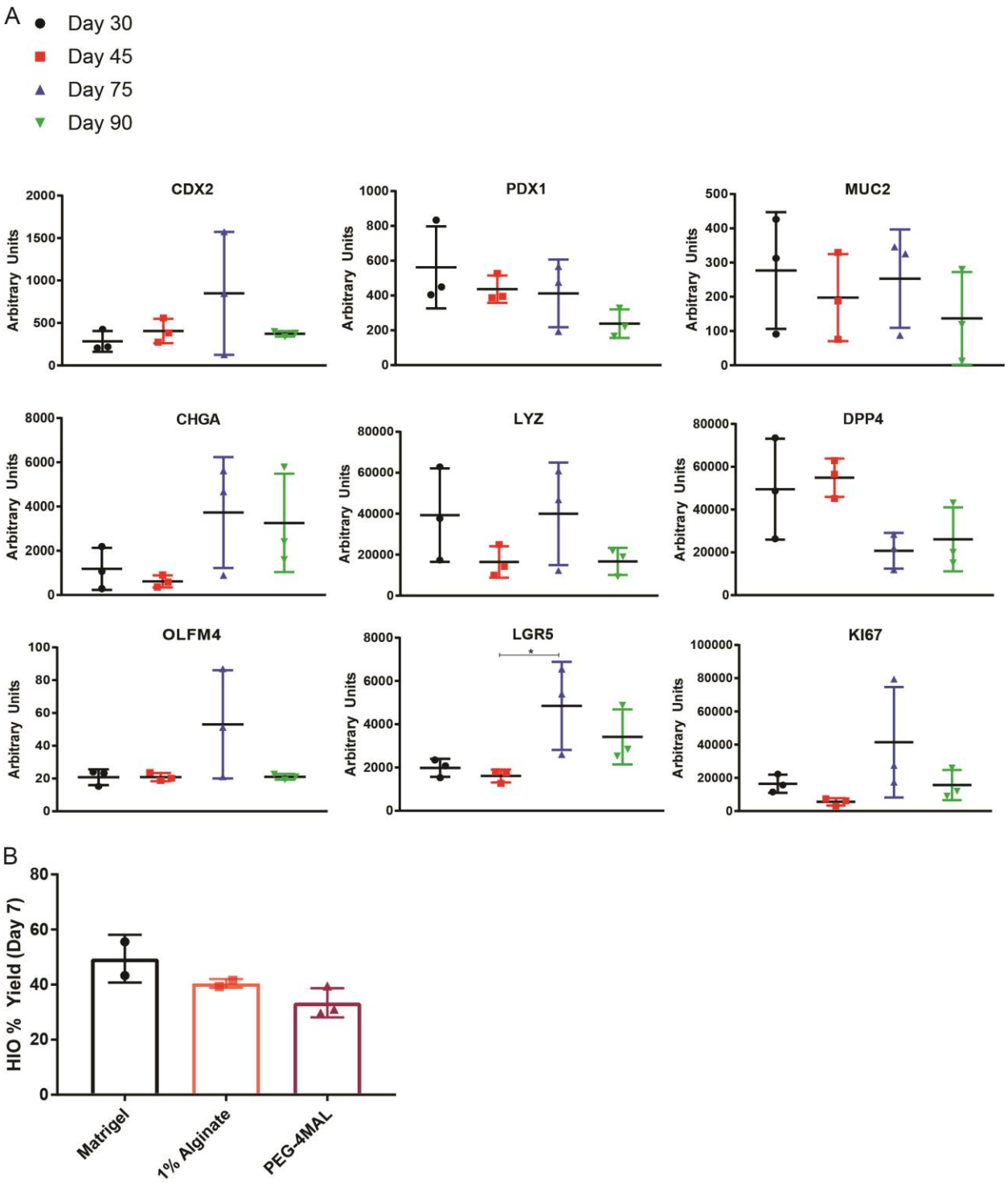

Figure S3. Further characterization of alginate-grown HIOs. Related to Figure 1. **(a)**: qRT-PCR analysis of CDX2, LGR5, PDX1, MUC2, CHGA, LYZ, DPP4, KI67, OLFM4, VIL1, and ZO-1 expression in HIOs cultured in 1% alginate over time for 90 days. Expression levels are normalized to ECAD to account for varying amounts of epithelium in HIOs. Each point is representative of 6-10 HIOs pooled from the same batch. Data represent the mean ± SE. Significance was calculated with a one-way ANOVA and Tukey's multiple comparisons test. The strength of p values is reported according the following: $p > 0.05$, $*p \leq 0.05$, $**p \leq 0.01$, $***p \leq 0.001$, $****p \leq 0.0001$. **(b):** Quantification of the percentage of spheroids which gave rise to organoids after 7 days of culture in Matrigel, 1% alginate, and 4% PEG-4MAL. Data shown are the average yields from 2 (alginate and Matrigel) or 3 (PEG-4MAL)

independent experiments with n>100 spheroids per condition. Each point depicts overall yield from one experiment, while bars depict mean and SE. Significance was calculated with a one-way ANOVA and Tukey's multiple comparisons test. The strength of p values is reported according the following: $p > 0.05$, $*p \leq 0.05$, $**p \leq 0.01$, $***p \leq 0.001$, $****p \leq 0.0001$.

Supplemental Experimental Procedures

hESC/hIPSC Lines and Generation of hPSC-Derived Intestinal Organoids

hPSC lines were induced to differentiate into endoderm using Activin A (100ng/mL, R & D Systems) for 3 days in RPMI1640 media supplemented with 0%, 0.2%, 2% HyClone dFBS on subsequent days. Endoderm was induced to differentiate into the intestinal lineage by treating cells for 5-6 days with FGF4 (500ng/mL, generated as previously described (Leslie et al., 2015)) and CHIR99021 (2μM). Following differentiation, free-floating hindgut spheroids were collected from differentiated stem cell cultures after days 5 and 6 of hindgut specification and plated in Matrigel (diluted with Advanced DMEM/F12 to a final protein concentration of 8 mg/mL) or alginate droplets as described in Experimental Procedures on a 24-well tissue culture grade plate. Organoid growth media consisted of Advanced DMEM/F12 supplemented with 1X B27 (Thermo Fisher, Waltham, MA), GlutaMAX (Gibco, 1X), penicillin-streptomycin (Gibco, 100 U ml^{-1} penicillin; 100 μg ml^{-1} streptomycin), HEPES buffer (Gibco, 15 mM), epidermal growth factor (EGF) (R&D Systems; 100 ng/mL), Noggin-Fc (100ng/mL) (purified from conditioned media (Heijmans et al., 2013)), and R-Spondin2 (5% conditioned medium (Bell et al., 2008)). Media was changed every 5-7 days.

Maintenance of HIOs

For studies of up to 30 days, alginate and Matrigel-grown HIOs were not passaged. For the 90-day study of alginate-grown HIOs, organoids were passaged in a similar manner to previously described methods for hydrogel or Matrigel-grown HIOs (Cruz-Acuna et al., 2017; Spence et al. 2011). Briefly, HIOs were dislodged from the alginate hydrogel by pipetting up and down and transferred to a sterile Petri dish. Excess alginate was removed by cutting it away with a scalpel, and HIOs were manually cut in half with a scalpel. HIO halves were transferred to fresh alginate solutions and re-embed in a clean 24-well tissue culture grade plate upon gelation with calcium chloride.

Epithelial Isolation

HIOs and tHIOs were incubated in dispase (07923; STEMCELL Technologies) for 30 minutes on ice. Following incubation, dispase was removed and replaced with 100% fetal bovine serum for 15 minutes on ice. To mechanically separate the epithelium from mesenchyme, a volume of advanced Dulbecco's modified Eagle medium/F12 (12634010; Gibco) equal to the initial volume of fetal bovine serum was added to the tissue before vigorously pipetting the mixture several times. Epithelial fragments then settled to the bottom where they were collected manually on a stereoscope by pipet. The epithelium was washed with ice-cold advanced Dulbecco's modified Eagle medium/F12 and allowed to settle to the bottom of a 1.5-mL Eppendorf tube. The media was then withdrawn from the loose tissue pellet and replaced with Matrigel on ice. The Matrigel containing the isolated epithelium was gently mixed to evenly suspend the cells before being pipetted into individual 50 μL droplets in a 24-well plate. The plate containing the droplets was incubated at 37°C for 15 minutes to allow the Matrigel to solidify before adding LWRN growth media containing Thiazovivin (2.5 μmol/L), SB431542 (100 nmol/L), CHIR99021 (4 μmol/L), and Y27632 (10 μmol/L). LWRN growth media was produced as previously described (Tsai et al., 2018). In summary, conditioned media from L-WRN cells containing Wnt3a, Rspondin3, and Noggin was mixed at a ratio of 1:1 with 2× basal media comprised of 214 mL advanced Dulbecco's modified Eagle medium/F12, 5 mL GlutaMAX (Gibco, Japan) (100×, 200 mmol/L), 5 mL HEPES (100×, 1 mol/L), 5 mL N2 supplement (100×), 10 mL B27 supplement (50×), 5 mL penicillin/streptomycin (100×), 1 mL N-acetylcystine (500 mmol/L), and 5 mL nicotinamide (1 mol/L). After 24 hours, the media was replaced with LWRN growth media containing TZV (2.5 μmol/L), SB431542 (100 nmol/L), and CHIR99021 (4 μmol/L). After 3 days, cultures were maintained with LWRN growth media replaced every other day.

RNA-sequencing and Bioinformatics Analysis

RNA from each sample was isolated using MagMAX-96 Total RNA (AM1830; Applied Biosystems) RNA isolation kits and used as input for library generation with Takara SMARTer Stranded Total RNA Sample Prep Kit (634876; Takara Bio USA). Samples were sequenced for 50-bp single-end reads across 10 lanes on an Illumina HiSeq 2500 by the University of Michigan DNA Sequencing Core. All reads were quantified using Kallisto pseudo alignment to an index of transcripts from all human genes within the Ensembl GRCh38 database (Bray et al., 2016). Gene level data generated from Kallisto was used to create normalized data matrix of pseudoaligned sequences (Transcripts Per

Million, TPM) and differential expression was calculated using the Bioconductor package DEseq2. Estimated counts per transcript using the Bioconductor package tximport. Differential expression analysis was performed using the Bioconductor package DESeq2 using gene count data (Love et al., 2014). A gene was considered to be differentially expressed if it had a 2-fold or larger difference between groups and an adjusted *P* value of .01 or less. Principal component analysis and sample clustering were performed in R with log2 transformed and centered gene counts of gene level data on all genes that had a sum of at least 10 counts across all samples. Replicates for all samples were clustered by Euclidian distance, and pairwise Pearson correlation coefficients were plotted in R. All reads are deposited at the EMBL-EBI ArrayExpress archive under accession E-MTAB-7000.

RNA Extraction and quantitative RT-PCR Analysis

qRT-PCR experiments were carried out as previously described (Miller et al., 2018). RNA was extracted using the MagMAX-96 Total RNA Isolation System (Life Technologies). RNA quality and concentration was assessed using a Nanodrop 2000 spectrophotometer (Thermo Scientific). Isolated RNA was used to generate a cDNA library using the SuperScript VILO cDNA master mix kit (Invitrogen) according to manufacturer's instructions. qRT-PCR analysis was conducted using Quantitect SYBR Green Master Mix (Qiagen) on a Step One Plus Real-Time PCR system (Life Technologies). Expression was calculated as a change relative to ECAD expression using arbitrary units, which were calculated by the following equation: [2^(ECAD Ct - Gene Ct)] x 10,000. Expression was normalized to ECAD as we analyzed epithelial-specific genes and there were variable levels of epithelium between samples. A Ct value of 40 or greater was considered not detectable. A list of primer sequences used can be found in the table below.

Primer Information

Gene Target	Forward Primer Sequence	Reverse Primer Sequence
GAPDH	CTCTGCTCCTCCTGTTCGAC	TTAAAAGCAGCCCTGGTGAC
ECAD	TTGACGCCGAGAGCTACAC	GACCGGTGCAATCTTCAAA
CDX2	GGGCTCTCTGAGAGGCAGGT	GGTGACGGTGGGGTTTAGCA
LGR5	CAGCGTCTTCACCTCCTACC	TGGGAATGTATGTCAGAGCG
PDX1	CGTCCGCTTGTTCTCCTC	CCTTTCCCATGGATGAAGTC
MUC2	TGTAGGCATCGCTCTTCTCA	GACACCATCTACCTCACCCG
CHGA	CTGTCCTGGCTCTTCTGCTC	TGACCTCAACGATGCATTTC
LYZ	ACAAGCTACAGCATCAGCGA	GTAATGATGGCAAAACCCCA
DPP4	TCCCGGTGGGAGTACTATGA	CAGGGCTTTGGAGATCTGAG
KI67	CAGGGCTTTGGAGATCTGAG	TGACTTCCTTCCATTCTGAAGAC
OLFM4	ACCTTTCCCGTGGACAGAGT	TGGACATATTCCCTCACTTTGGA
VIL1	CCAAAGGCCTGAGTGAAATC	CCTGGAGCAGCTAGTGAACA
ZO-1	GGGAACAACATACAGTGACGC	CCCCACTCTGAAAATGAGGA

Note: All primer sequences were obtained from http://primerdepot.nci.nih.gov. All annealing temperatures are near 60°C.

Culture of Intestinal Epithelium and Intestinal Mesenchyme

Human fetal intestinal enteroids were generated by isolating the crypts from human fetal intestinal tissue and expanding them in Matrigel droplets as previously described (Tsai et al., 2018). Intestinal mesenchyme was isolated from human fetal duodenum that was separated from the epithelium and expanded in culture. For co-culture experiments, small enteroids were mechanically removed from Matrigel 3 days after passaging. Mesenchyme was passaged into single cells and counted using a hemocytometer. Enteroids were suspended in 10 µL droplets of LWRN medium on the bottom of a tissue culture dish with 1 enteroid per droplet. 2,000 mesenchymal cells were added to each droplet for a total droplet volume of no more than 20 µL. After placing the lid onto the plate, the plate was flipped upside down to establish hanging drop co-cultures. The plate containing hanging drops was floated in a larger tissue culture plate containing sterile PBS and left in a tissue culture incubator overnight for 16 hours to allow for aggregation of epithelium with mesenchyme. The plate containing the hanging drops was then quickly flipped to an upright

position. Co-culture aggregates were carefully removed by pipetting and suspended in 1% alginate and Matrigel solutions. Cultures were maintained for up to 10 days. LWRN medium was changed approximately every 3 days.

Antibody Information

Primary Antibody	Source	Catalog #	Dilution
Goat anti-E-cadherin	R&D Systems	af748	1:500
Mouse anti-E-cadherin	BD Transduction Laboratories	610181	1:500
Goat anti-Vimentin	R&D Systems	mab2105	1:500
Mouse anti-CDX2	BioGenex	MU392A-UC	1:300
Rabbit anti-PDX1	Epitomics, Inc	3470-1	1:300
Rabbit anti-ZO-1	Cell Signaling	13663	1:300
Rabbit anti-MUC2	Santa Cruz Biotechnology	sc-15334	1:300
Goat-anti CHGA	Santa Cruz Biotechnology	sc-1488	1:300
Goat-anti SOX9	R&D Systems	af3075	1:300
rabbit-anti KI67	Thermo Scientific	RM-9106-S1	1:300
Goat-anti DPP4	R&D Systems	af954	1:300
Goat-anti LYZ	Santa Cruz Biotechnology	sc-27958	1:300
Rabbit-anti DEFA5	Abcam	ab180515	1:300
Rabbit-anti OLFM4	Abcam	ab85046	1:300
Rabbit-anti LGR5	Abcam	ab75850	1:300
Goat-anti Villin	Santa Cruz	sc-7672	1:300

Supplemental References

1. Bell, S., Schreiner, C., Wert, S., Mucenski, M., Scott, W., Whitsett, J., 2008. R-spondin 2 is required for normal laryngeal-tracheal, lung and limb morphogenesis. Development 135, 1049-1058.
2. Bray, N.L., Pimental, H., Melsted, P., Pachter, L., 2016. Near-optimal probabilistic RNA-seq quantification. Nature Biotechnology 34, 525-527.
3. Heijmans, J., van Lidth de Jeude, J., Koo, B., Rosekrans, S., Wielenga, M., van de Wetering, M., Ferrante, M., Lee, A., Onderwater, J., Paton, J., Paton, A., Mommaas, A., Kodach, L., Hardwick, J., Hommes, D., Clevers, H., Muncan, V., van den Brink, G., 2013. ER stress causes rapid loss of intestinal epithelial stemness through activation of the unfolded protein response. Cell Rep 3, 1128-1139.
4. Leslie, J., Huang, S., Opp, J., Nagy, M.S., Kobayashi, M., Young, V.B., Spence, J.R., 2015. Persistence and toxin production by Clostridium difficile within human intestinal organoids result in disruption of epithelial paracellular barrier function. Infection and Immunity 83, 138-145.
5. Love, M.I., Huber, W., Anders, S., 2014. Moderated estimation of fold change and dispersion for RNA-seq with DESeq2. Genome Biology 15:550.